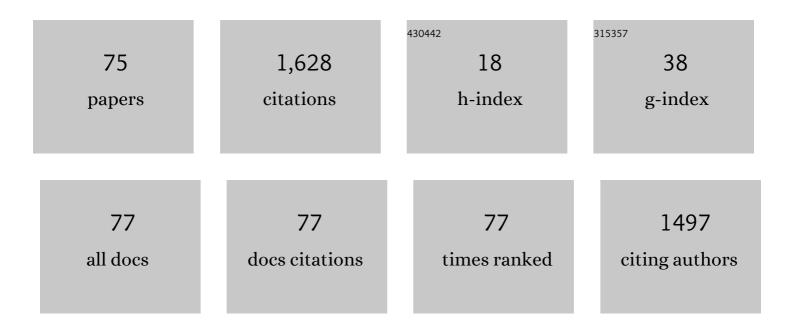


## List of Publications by Year in descending order

Source: https://exaly.com/author-pdf/4161329/publications.pdf Version: 2024-02-01



V<sub>A</sub>O Lu

#	Article	IF	CITATIONS
1	Structural Characterization of Lignin and Its Degradation Products with Spectroscopic Methods. Journal of Spectroscopy, 2017, 2017, 1-15.	0.6	201
2	Ultrahigh power factor and flexible silver selenide-based composite film for thermoelectric devices. Energy and Environmental Science, 2020, 13, 1240-1249.	15.6	165
3	Good Performance and Flexible PEDOT:PSS/Cu <sub>2</sub> Se Nanowire Thermoelectric Composite Films. ACS Applied Materials & Interfaces, 2019, 11, 12819-12829.	4.0	153
4	Ultrahigh Performance of n-Type Ag <sub>2</sub> Se Films for Flexible Thermoelectric Power Generators. ACS Applied Materials & Interfaces, 2020, 12, 9646-9655.	4.0	115
5	Ultrahigh performance polyvinylpyrrolidone/Ag2Se composite thermoelectric film for flexible energy harvesting. Nano Energy, 2021, 80, 105488.	8.2	82
6	Preparation and Characterization of Te/Poly(3,4-ethylenedioxythiophene):Poly(styrenesulfonate)/Cu <sub>7</sub> Te <sub>4</sub> Ternary Composite Films for Flexible Thermoelectric Power Generator. ACS Applied Materials & Interfaces, 2018, 10, 42310-42319.	4.0	74
7	Progress on PEDOT:PSS/Nanocrystal Thermoelectric Composites. Advanced Electronic Materials, 2019, 5, 1800822.	2.6	70
8	Characterization of a bio-oil from pyrolysis of rice husk by detailed compositional analysis and structural investigation of lignin. Bioresource Technology, 2012, 116, 114-119.	4.8	62
9	High Power Factor Ag/Ag <sub>2</sub> Se Composite Films for Flexible Thermoelectric Generators. ACS Applied Materials & Interfaces, 2021, 13, 14327-14333.	4.0	58
10	Enhanced-Performance PEDOT:PSS/Cu <sub>2</sub> Se-Based Composite Films for Wearable Thermoelectric Power Generators. ACS Applied Materials & Interfaces, 2021, 13, 631-638.	4.0	49
11	Exceptionally High Power Factor Ag <sub>2</sub> Se/Se/Polypyrrole Composite Films for Flexible Thermoelectric Generators. Advanced Functional Materials, 2022, 32, 2106902.	7.8	49
12	Exceptional power factor of flexible Ag/Ag2Se thermoelectric composite films. Chemical Engineering Journal, 2022, 434, 134739.	6.6	33
13	Giant enhancement of THz-frequency optical nonlinearity by phonon polariton in ionic crystals. Nature Communications, 2021, 12, 3183.	5.8	29
14	Paint Removal on the 5A06 Aluminum Alloy Using a Continuous Wave Fiber Laser. Coatings, 2019, 9, 488.	1.2	25
15	Air-Core Ring Fiber With >1000 Radially Fundamental OAM Modes Across O, E, S, C, and L Bands. IEEE Access, 2020, 8, 68280-68287.	2.6	23
16	Simultaneous quantification of eleven bioactive phenolic compounds in pigeon pea natural resources and in vitro cultures by ultra-high performance liquid chromatography coupled with triple quadrupole mass spectrometry (UPLC-QqQ-MS/MS). Food Chemistry, 2021, 335, 127602.	4.2	21
17	Polarization-resolved edge states in terahertz topological photonic crystal. Optics Express, 2019, 27, 22819.	1.7	21
18	Simultaneous determination of taxoids and flavonoids in twigs and leaves of three Taxus species by UHPLC-MS/MS. Journal of Pharmaceutical and Biomedical Analysis, 2020, 189, 113456.	1.4	20

#	Article	IF	CITATIONS
19	Design guidelines for chalcogenide-based flexible thermoelectric materials. Materials Advances, 2021, 2, 2584-2593.	2.6	18
20	Analytical Strategies Involved in the Detailed Componential Characterization of Biooil Produced from Lignocellulosic Biomass. International Journal of Analytical Chemistry, 2017, 2017, 1-19.	0.4	17
21	Outage Probability of Cooperative Relay Networks in Two-Wave with Diffuse Power Fading Channels. IEEE Transactions on Communications, 2012, 60, 42-47.	4.9	16
22	Porous nanocomposite membranes based on functional GO with selective function for lithium adsorption. New Journal of Chemistry, 2018, 42, 4432-4442.	1.4	16
23	Giant Tunable Circular Dichroism of Large-Area Extrinsic Chiral Metal Nanocrescent Arrays. Nanoscale Research Letters, 2019, 14, 388.	3.1	16
24	Ultraviolet laser cleaning and surface characterization of AH36 steel for rust removal. Journal of Laser Applications, 2020, 32, .	0.8	15
25	Application of UV-B radiation for enhancing the accumulation of bioactive phenolic compounds in pigeon pea [Cajanus cajan (L.) Millsp.] hairy root cultures. Journal of Photochemistry and Photobiology B: Biology, 2022, 228, 112406.	1.7	14
26	Effective Production of Phenolic Compounds with Health Benefits in Pigeon Pea [Cajanus cajan (L.) Millsp.] Hairy Root Cultures. Journal of Agricultural and Food Chemistry, 2020, 68, 8350-8361.	2.4	13
27	Topological Valley Transport of Terahertz Phonon–Polaritons in a LiNbO <sub>3</sub> Chip. ACS Photonics, 2021, 8, 2737-2745.	3.2	13
28	A comparison of autologous transplantation of retinal pigment epithelium ( <scp>RPE</scp> ) monolayer sheet graft with <scp>RPE</scp> –Bruch's membrane complex graft in neovascular ageâ€related macular degeneration. Acta Ophthalmologica, 2017, 95, e443-e452.	0.6	12
29	Interface energy level alignment and improved film quality with a hydrophilic polymer interlayer to improve the device efficiency and stability of all-inorganic halide perovskite light-emitting diodes. Journal of Materials Chemistry C, 2020, 8, 6743-6748.	2.7	12
30	Topologically tuned terahertz confinement in a nonlinear photonic chip. Light: Science and Applications, 2022, 11, .	7.7	12
31	Symbol Error Rate of Decode-and-Forward Relaying in Two-Wave with Diffuse Power Fading Channels. IEEE Transactions on Wireless Communications, 2012, 11, 3412-3417.	6.1	11
32	Zwitterion imprinted composite membranes with obvious antifouling character for selective separation of Li ions. Korean Journal of Chemical Engineering, 2020, 37, 707-715.	1.2	11
33	Evaluation of coalâ€related model compounds using tandem mass spectrometry. Rapid Communications in Mass Spectrometry, 2018, 32, 1462-1472.	0.7	10
34	Development of the inorganic nanoparticles reinforced alginateâ€based hybrid fiber for wound care and healing. Journal of Applied Polymer Science, 2021, 138, 51228.	1.3	10
35	On-chip plasmon-induced transparency in THz metamaterial on a LiNbO3 subwavelength planar waveguide. Optics Express, 2019, 27, 7373.	1.7	10
36	ldentification of genes associated with biosynthesis of bioactive flavonoids and taxoids in Taxus cuspidata Sieb. et Zucc. plantlets exposed to UV-B radiation. Gene, 2022, 823, 146384.	1.0	10

#	Article	IF	CITATIONS
37	Preparation of a polylactic acid knitting mesh for pelvic floor repair and in vivo evaluation. Journal of the Mechanical Behavior of Biomedical Materials, 2017, 74, 204-213.	1.5	9
38	Hollow Ring-Core Photonic Crystal Fiber With >500 OAM Modes Over 360-nm Communications Bandwidth. IEEE Access, 2021, 9, 66999-67005.	2.6	9
39	Adaptive bayesian beamforming with sidelobe constraint. IEEE Communications Letters, 2010, 14, 369-371.	2.5	8
40	The dark current suppression of black silicon photodetector by a lateral heterojunction. Optical Materials, 2020, 110, 110474.	1.7	8
41	Conversion from terahertz-guided waves to surface waves with metasurface. Optics Express, 2018, 26, 31233.	1.7	8
42	Suppressed Halide Segregation and Defects in Wide Bandgap Perovskite Solar Cells Enabled by Doping Organic Bromide Salt with Moderate Chain Length. Journal of Physical Chemistry C, 2022, 126, 1711-1720.	1.5	8
43	Surface enhancement of THz wave by coupling a subwavelength LiNbO3 slab waveguide with a composite antenna structure. Scientific Reports, 2017, 7, 17602.	1.6	7
44	Propagation of THz pulses in rectangular subwavelength dielectric waveguides. Journal of Applied Physics, 2018, 123, .	1.1	7
45	Solvent modification to suppress halide segregation in mixed halide perovskite solar cells. Journal of Materials Science, 2020, 55, 9787-9794.	1.7	7
46	Predictors of short-term outcomes related to central subfield foveal thickness after intravitreal bevacizumab for macular edema due to central retinal vein occlusion. International Journal of Ophthalmology, 2016, 9, 86-92.	0.5	7
47	Bentonite–Acrylamide Hydrogels Prepared by the Nonmixing Method: Characterization and Properties. ACS Omega, 2019, 4, 16826-16832.	1.6	6
48	SRSF5 regulates alternative splicing of DMTF1 pre-mRNA through modulating SF1 binding. RNA Biology, 2021, , 1-19.	1.5	6
49	Efficient generation and frequency modulation of quasi-monochromatic terahertz wave in Lithium Niobate subwavelength waveguide. Optics Express, 2017, 25, 14766.	1.7	5
50	Observation of "Frozenâ€Phase―Propagation of THz Pulses in a Dispersive Optical System. Laser and Photonics Reviews, 2021, 15, 2000591.	4.4	5
51	Fabrication, characterization and application of polypropylene macroporous mesh for repairing pelvic floor defects. Textile Reseach Journal, 2017, 87, 878-888.	1.1	4
52	Time-resolved imaging of mode-conversion process of terahertz transients in subwavelength waveguides. Frontiers of Physics, 2019, 14, 1.	2.4	4
53	A Novel Evaluation Method Developed for the Denitrogenation and Deoxygenation on Molecules in Coal during Catalytic Treatments. ChemistrySelect, 2019, 4, 13582-13588.	0.7	4
54	Cavity-cavity coupling based on a terahertz rectangular subwavelength waveguide. Journal of Applied Physics, 2019, 126, 063103.	1.1	3

#	Article	IF	CITATIONS
55	Giant nonlinearity of THz waves mediated by photon-phonon strong coupling. , 2020, , .		3
56	In-plane reflection phase engineering of graphene plasmons realized by electronic boundary design at the nanoscale. AIP Advances, 2022, 12, .	0.6	3
57	Health-Promoting Phenolic Compound Accumulation, Antioxidant Response, Endogenous Salicylic Acid Generation, and Biosynthesis Gene Expression in Germinated Pigeon Pea Seeds Treated with UV-B Radiation. Journal of Agricultural and Food Chemistry, 2022, 70, 5680-5690.	2.4	3
58	OPTIC DISK ASTROCYTOMA UNASSOCIATED WITH TUBEROUS SCLEROSIS COMPLEX MANAGED WITH SURGICAL EXCISION AND A 7-YEAR FOLLOW-UP. Retinal Cases and Brief Reports, 2018, Publish Ahead of Print, 462-467.	0.3	2
59	Insight into molecular information of Huolinguole lignite obtained by Fourier transform ion cyclotron resonance mass spectrometry and statistical methods. Rapid Communications in Mass Spectrometry, 2019, 33, 1107-1113.	0.7	2
60	Device performance improvements in all-inorganic perovskite light-emitting diodes: the role of binary ammonium cation terminals. Physical Chemistry Chemical Physics, 2022, 24, 6208-6214.	1.3	2
61	Outage Probability of Cooperative Relay Systems in Two-Wave with Diffuse Power Fading Environments. , 2011, , .		1
62	Asymptotic Performance Analysis of AF Relaying in Two-Wave with Diffuse Power Fading Channels. , 2012, , .		1
63	Cathodoluminescence Enhancement of MoS <sub>2</sub> by Femtosecond Laser Induced Periodic Surface Structures. Journal of Nanoscience and Nanotechnology, 2018, 18, 7557-7560.	0.9	1
64	Transient establishment of the wavefronts for negative, zero, and positive refraction. Optics Express, 2018, 26, 1954.	1.7	1
65	Terahertz Integration and Spatio-Temporal Super-Resolution Imaging on LiNbO3 Chip. Zhongguo Jiguang/Chinese Journal of Lasers, 2019, 46, 0508003.	0.2	1
66	THz Nonlinearity Enhancement by Phonon Polaritons in Ionic Crystals. , 2021, , .		0
67	Real-space and real-time imaging of THz wave confinement and standing wave in a Fabry-Perot resonator. , 2017, , .		0
68	10.1063/1.5030515.1., 2018, , .		0
69	Repair of pseudo time-reversal broken by topological phase transition in a photonic crystal slab. , 2019, , .		0
70	On-chip plasmon-induced transparency using a meta-structure in THz regime. , 2019, , .		0
71	Visualization of a cavity-cavity coupling in a LiNbO3 subwavelength waveguide at THz frequency. , 2019, , .		0

#	Article	IF	CITATIONS
73	Propagation phase elimination of light pulses by an initial phase-locked synchronized moving source. , 2020, , .		0
74	Demonstration of highly unidirectional edge states in terahertz slab waveguides. , 2020, , .		0
75	A Study on Data-Driven Novel Cancer Staging Methods. Studies in Health Technology and Informatics, 2017, 245, 1263.	0.2	0